Sensors and Materials, Vol. 18, No. 5 (2006) 261–275
MYU Tokyo

S & M 0648

Evaluation of Gauge Coefficients for Modelling Piezoresistive Properties of Thick-Film Resistors

Marina Santo Zarnik[1,2,*], Darko Belavič[2] and Artur Wymysłowski[3]

[1]Electronic Ceramics Department, Jozef Stefan Institute, Jamova 39, SI-1000 Ljubljana, Slovenia
[2]HIPOT-R&D, Trubarjeva 7, 8310 Šentjernej, Slovenia
[3]Wroclaw University of Technology, ul. Grabiszńyska 97, 53-439 Wroclaw, Poland

(Received November 11, 2005; accepted May 2, 2006)

***Key words*:** piezoresistivity, thick-film resistor, gauge factor, gauge coefficients, finite-element model

The piezoresistive properties of thick-film resistors have been utilized for strain gauges and related sensor applications for many years. In spite of the accumulated knowledge of the phenomenon and the wide experience in designing various sensor structures, it is still a challenge to build a numerical model that provides good agreement between numerical simulations and experimental results. The main problem with numerical modelling is not only the proper formulation of the effect in terms of the material parameters relating to the electrical field and the strain components in the deformed resistor body but, primarily, the experimental evaluation of those parameters for the selected thick-film resistor material. In this paper, we present an experimental and mathematical procedure for evaluating thick-film piezoresistor model parameters and discuss the results obtained for two commercial thick-film resistor materials printed and fired on different ceramic substrates. As a validation, the results of the simulations were compared with measurements of specially designed test patterns that were not used for the evaluation of the gauge coefficients.

1. Introduction

Thick-film resistors are widely used as sensing elements in ceramic micro-electro-mechanical systems (C-MEMSs) because of the relatively high sensitivity of their resistance to an applied mechanical load.[(1)] In spite of the accumulated knowledge of the phenomenon and practical experiences in designing such systems, there is an enormous interest in simplifying this demanding and time-consuming task. Following a traditional design approach, which involves extensive physical testing, several iterative design steps are generally needed before the prototypes are ready for serial production. A promising strategy for reducing the number of design cycles and thereby decreasing the development time and cost, is the use of numerical simulations. In a simulation-based design strategy, an accurate modelling of the sensing thick-film resistors is essential if we are to achieve useful

*Corresponding author, e-mail address: marina.santo@ijs.si

results from simulations. Although the piezoresistivity of thick-film resistors has been studied for many years,[2-12] it is still a challenge to specify the material parameters in an appropriate form that can be used in a simulation-based analysis. The traditional approach to evaluating the piezoresistance effect of thick-film resistors involves measuring the resistor's sensitivity to strain, the so-called gauge factor (*GF*), which is defined as the ratio of the fractional change in resistance to the strain in the resistor body as a result of an applied mechanical load. In the case of numerical modelling, we are interested in the resistivity changes rather than the resistance changes.[2,13–15] For this reason, physical quantities, i.e., coefficients relating the resistivity to the strain components in the relationship between electrical field strength and current density have to be evaluated. These parameters are called "gauge coefficients" by analogy with the term gauge factor, since both parameters describe the sensitivity to strain. The separation of the geometrical and physical contributions to the strain sensitivity of thick-film resistors was discussed many years ago. The relationships between the gauge coefficients and the measured *GF*s, which were derived for isotropic materials in ref. 2, revealed that considerable differences between these two values may occur.

In this paper, we focus on an experimental and mathematical procedure for evaluating the gauge coefficients relating the strain components to the electrical field strength and the current density in the constitutional equation for the thick-film piezoresistive structure. In the first part, the mathematical formulation of the piezoresistive effect in the thick-film resistor is discussed, and the expressions for calculating the gauge coefficients are derived. The relationships are determined on the basis of the facts that thick-film resistors can exhibit anisotropic sensitivity to strain and that the elasticity properties of the resistor can differ from the properties of the ceramic substrate. The results obtained for different combinations of thick-film resistors and ceramic substrate materials are discussed. As a validation of the evaluation procedure and the FE model, the simulation results were compared with the values obtained from measuring the specially designed test patterns.

2. Piezoresistive Effect in Thick-Film Resistors

2.1 *Piezoresistance and piezoresistivity phenomenon*

Two terms are commonly used to describe the piezoresistive properties of resistors: piezoresistance and piezoresistivity. The piezoresistance, which is described by the gauge factor, refers to resistance changes, while the piezoresistivity refers to a material property and is defined as the change in the bulk resistivity ρ due to the appropriate strain component.

The gauge factor (*GF)* is commonly defined by the relation

$$GF = \frac{dR/R}{\varepsilon}, \tag{1}$$

where dR/R is the relative change in the resistance and ε is the strain along the length of the resistor, defined as the relative change in the length (l), $\varepsilon = dl/l$.

On the basis of resistor's orientation and with respect to the direction of the dominant strain component (ε), the longitudinal gauge factor (GF_L) and the transverse gauge factor (GF_T) are defined as

$$GF_L = \frac{dR_L / R_L}{\varepsilon} = \frac{dR_L / R_L}{dl / l}, \quad GF_T = \frac{dR_T / R_T}{\varepsilon} = \frac{dR_T / R_T}{dw / w}, \tag{2}$$

where R_L and R_T denote longitudinally and transversally oriented resistors. GF_L is measured in the case when the electrical current through the resistor is parallel to the applied strain, and GF_T is measured in the case when the current is perpendicular to the strain. The situation is schematically shown in Fig. 1.

In the case of a homogenous resistive material and the conventional rectangular shape of a thick-film resistor, its resistance is governed by the well-known analytical expression

$$R = \rho \frac{l}{wt}, \tag{3}$$

where ρ is the bulk resistivity, l is the length, w is the width, and t is the thickness of the resistor. When the resistor is uniaxially strained along its length, the resistance change can be evaluated by a logarithmic differentiation of eq. (3), which leads to the relation

$$\frac{dR}{R} = \frac{d\rho}{\rho} + \frac{dl}{l} - \frac{dw}{w} - \frac{dt}{t}, \tag{4}$$

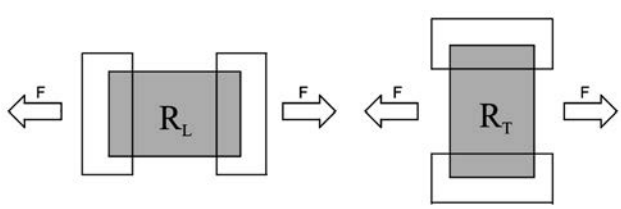

(a) (b)

Fig. 1. Orientation of thick-film resistor with respect to direction of applied strain: (a) longitudinally oriented resistor, R_L, aimed at evaluation of GF_L and (b) transversally oriented resistor, R_T, used for evaluation of GF_T (right).

where the terms dl/l, dw/w, and dt/t represent the fractional changes in the resistor's length, width and thickness, respectively. By replacing the relative change in dimensions with the appropriate strain component and Poisson's ratio v, i.e., $dl/l=\varepsilon$, $dw/w=-v\cdot\varepsilon$, $dt/t=-v\cdot\varepsilon$, eq. (4) can be rewritten as

$$\frac{dR}{R}=\frac{d\rho}{\rho}+\varepsilon\cdot(1+2v). \tag{5}$$

The above relationship, which in actual fact describes the piezoresistance phenomena, consists of two terms: the term $d\rho/\rho$, which is related to the material properties describing the piezoresistivity effect, and the term $\varepsilon\cdot(1+2v)$, representing the geometrical effect.

In the case of numerical modelling, we are interested in the material properties, which are independent of geometrical effects and can be specified in an appropriate form in accordance with the mathematical formulation of the phenomena. The separation of the geometrical and physical contributions to the strain sensitivity of thick-film resistors has been previously discussed in ref. 2, where the relationship between the measured gauge factors, GF_L and GF_T, and the gauge coefficients was derived assuming isotropic material properties.

2.2 *Mathematical formulation of piezoresistivity phenomena*

The mathematical formulation of the piezoresistivity effect is derived from the general relation governing the electric field strength and the current density in a conductor:

$$J=\sigma\cdot E=-\sigma\nabla U, \tag{6}$$

where J and E are the current-density and the electric-field-strength vectors, respectively, and σ represents the material conductivity.

If there is no source of charge inside the resistor the potential distribution and the resulting current flow are governed by

$$\nabla\cdot J+\frac{\partial D}{\partial t}=0, \tag{7}$$

where D is the charge density.

Since we shall be dealing with static phenomena, the time derivative in eq. (6) is zero, and combining eqs. (6) and (7) results in the relation governing the electrical conduction in the resistor:

$$\nabla\cdot J=-\nabla\cdot(\sigma\nabla U)=0. \tag{8}$$

The solution of eq. (8) gives the current density and potential distribution in the resistor body. By integrating the current density over the entire cross section of the resistor, the

total current, I, flowing through the resistor can be obtained. The resistance, R, can then be calculated using Ohm's law, $R=\Delta U/I$, where ΔU is the voltage applied to the connection pads of the resistor.

Observing the problem in a cubic orthogonal system (1–3), the relation between the current density and the electrical field strength can be rewritten in matrix form as

$$\begin{bmatrix} E_1 \\ E_2 \\ E_3 \end{bmatrix} = \begin{bmatrix} \rho_{11} & \rho_{12} & \rho_{13} \\ \rho_{21} & \rho_{22} & \rho_{23} \\ \rho_{31} & \rho_{32} & \rho_{33} \end{bmatrix} \cdot \begin{bmatrix} j_1 \\ j_2 \\ j_3 \end{bmatrix}, \tag{9}$$

where E_i and j_i are the electric-field-strength and current-density components, and $[\rho]$ is the resistivity tensor. For an unstrained resistor made of an isotropic, resistive material, only the coefficients $\rho_{11} = \rho_{22} = \rho_{33} = \rho$ have a nonzero value. In the case of a mechanical load, which strains the resistor, eq. (9) changes to

$$\begin{bmatrix} E_1 \\ E_2 \\ E_3 \end{bmatrix} = \begin{bmatrix} \rho + \Delta\rho_{11} & \Delta\rho_{12} & \Delta\rho_{13} \\ \Delta\rho_{21} & \rho + \Delta\rho_{22} & \Delta\rho_{23} \\ \Delta\rho_{31} & \Delta\rho_{32} & \rho + \Delta\rho_{33} \end{bmatrix} \cdot \begin{bmatrix} j_1 \\ j_2 \\ j_3 \end{bmatrix}, \tag{10}$$

where ρ is the resistivity of the mechanically unloaded resistor, and $\Delta\rho_{ii}$ represents increments due to the piezoresistivity effect.

The piezoresistivity effect is generally described by the relationship between the resistivity and the strain components in which the gauge coefficients are specified as a tensor of rank 4, which contains, in the most general case, 36 components. In practice, there is no need to fully define all the components of the piezoresistive tensor. In formulations derived for silicon and germanium single-crystal symmetry, only three independent piezoresistive coefficients are required to fully define the piezoresistive properties of the material. The formulation of the piezoresistive effect in polycrystalline aggregates (spherical symmetry), such as thick-film resistors, had been proposed in refs. 4 and 5, for which only two linearly independent elements are required to populate the piezoresistance matrix. Using a similar formulation for the reduced matrix of the gauge coefficients, the resistivity changes in a thick-film piezoresistor can be expressed by

$$\frac{1}{\rho} \cdot \begin{bmatrix} \Delta\rho_{11} \\ \Delta\rho_{22} \\ \Delta\rho_{33} \\ \Delta\rho_{12} \\ \Delta\rho_{13} \\ \Delta\rho_{23} \end{bmatrix} = \begin{bmatrix} g_{11} & g_{12} & g_{13} & 0 & 0 & 0 \\ g_{21} & g_{22} & g_{23} & 0 & 0 & 0 \\ g_{31} & g_{32} & g_{33} & 0 & 0 & 0 \\ 0 & 0 & 0 & g_{44} & 0 & 0 \\ 0 & 0 & 0 & 0 & g_{55} & 0 \\ 0 & 0 & 0 & 0 & 0 & g_{66} \end{bmatrix} \cdot \begin{bmatrix} \varepsilon_{11} \\ \varepsilon_{22} \\ \varepsilon_{33} \\ \gamma_{12} \\ \gamma_{13} \\ \gamma_{32} \end{bmatrix}, \tag{11}$$

where g_{ij} denotes the gauge coefficients, ε_{ij} are the strain components, and γ_{ij}, $i \neq j$, are the shear-strain components.

Equation (11) can be simply coded in a finite element. The main challenge with modelling the piezoresistivity effect in thick-film resistors remains the evaluation of the gauge coefficients. A problem arises because the films change their resistance with induced strain in the substrate and only resistance changes, i.e., longitudinal and transversal *GF*s, can be measured directly. The proper material tensor can only be assessed with a certain accuracy by a separation from the measurable quantities. For this reason, some further assumptions and simplifications were made in our evaluation procedure, as described below.

2.3 *Evaluation of gauge coefficients*

Assuming the same values for the gauge coefficients, $g_{11}=g_2=g_{33}$ and $g_{12}=g_{21}$ and $g_{13}=g_{31}$, and that the influence of shear strain can be neglected (this is acceptable in many cases in practice), eq. (11) can be reduced to a system of three linear equations:

$$\begin{aligned}\Delta\rho_{11} &= \rho\cdot(g_{11}\cdot\varepsilon_{11} + g_{12}\cdot\varepsilon_{22} + g_{13}\cdot\varepsilon_{33})\\ \Delta\rho_{22} &= \rho\cdot(g_{12}\cdot\varepsilon_{11} + g_{11}\cdot\varepsilon_{22} + g_{13}\cdot\varepsilon_{33}),\\ \Delta\rho_{33} &= \rho\cdot(g_{13}\cdot\varepsilon_{11} + g_{12}\cdot\varepsilon_{22} + g_{11}\cdot\varepsilon_{33})\end{aligned} \tag{12}$$

where ε_{11}, ε_{22}, ε_{33} are the strain components in the longitudinal, transverse and third orthogonal directions, respectively.

To determine the gauge coefficients from eq. (12), three independent measurements are required. To avoid the difficult measurements of the strain sensitivity of the thick-film resistors in the third orthogonal direction and, in this way, simplify the evaluation procedure, we assumed that both transverse gauge coefficients g_{12} and g_{13} have the same value. (Considering macroscopic material properties, this can be a reasonable assumption because a thick-film resistor is made of a composite material with the conductive grains in an isolating, glassy matrix with the same microstructure in any transverse cross section and, therefore, we would expect the same mechanisms for conduction in both directions perpendicular to the direction of the electrical field and the current through the resistor.) In this way, the matrix of the gauge coefficients can be reduced to only two different coefficients, i.e., g_{11} and g_{12}. By denoting g_{11} as the longitudinal gauge coefficient, i.e., $g_{11}=g_l$, and the coefficients $g_{12}=g_{13}=g_t$ as the transversal gauge coefficients, the resistivity of the thick-film resistor can be finally specified as a function of the bulk resistivity of the mechanically unloaded resistor and the longitudinal and transversal gauge coefficients according to

$$\begin{aligned}\Delta\rho_{11} &= \rho + \rho\cdot(g_l\varepsilon_{11} + g_t\varepsilon_{22} + g_t\varepsilon_{33})\\ \Delta\rho_{22} &= \rho + \rho\cdot(g_l\varepsilon_{22} + g_t\varepsilon_{11} + g_t\varepsilon_{33}),\\ \Delta\rho_{33} &= \rho + \rho\cdot(g_l\varepsilon_{33} + g_t\varepsilon_{11} + g_t\varepsilon_{22})\end{aligned} \tag{13}$$

where ρ_{11}, ρ_{22}, and ρ_{33} represent the resistivity in the longitudinal, transverse, and third orthogonal directions, respectively.

The experimental procedure for estimating the *GF*s involves straining specially designed test patterns, i.e., ceramic substrates with appropriately positioned and oriented

thick-film resistors, and then measuring the resistance changes. Cantilever or bridge methods are generally applied for this purpose. Depending on the selected method, an appropriate measurement setup and test patterns are designed. Since the experimental values of the *GF*s depend to some extent on the measurement method and the design of the test patterns, it is important to ensure consistent experimental and mathematical evaluation procedures. As an example, a procedure for measuring gauge factors using the four-point bridge measurement method is described in ref. 6. In our particular case study, a three-point bending experimental setup was used and is schematically shown in Fig. 2.

The evaluation of the *GF*s for different thick-film resistive materials and substrates has been previously described in refs. 9 and 10. Here, the relationships for calculating the gauge coefficients from measurements accomplished using the same experimental set-up and test patterns of the same design are derived as follows.

Observing the test patterns in the Cartesian coordinate system, which is aligned so that the coordinate x corresponds to the longitudinal orientation (along the length of the longitudinally oriented resistor), and stretching the substrate in the longitudinal direction result in the dominant (longitudinal) strain component $\varepsilon = \varepsilon_{xx}$, and the perpendicular strain components ε_{yy} and ε_{zz}, which can be expressed by the relations

$$\varepsilon_{yy} = -\nu_c \cdot \varepsilon_{xx}, \quad \varepsilon_{zz} = -\nu_r \cdot \varepsilon_{xx} \ , \tag{14}$$

where ν_c and ν_r are the Poisson's ratios of the ceramic substrate and resistor material, respectively.

Assuming that the Young's modulus for the ceramic substrate is equal to or larger than that for the thick-film resistor, the strains of the resistor in the longitudinal and transverse directions are forced to be equal to the strains on the surface of the substrate in these directions. The strain component in the third orthogonal direction depends on the Poisson's ratio of the resistor material. Under such conditions and in accordance with the situation presented in Fig. 1, the relation governing the changes in the resistance of the strained

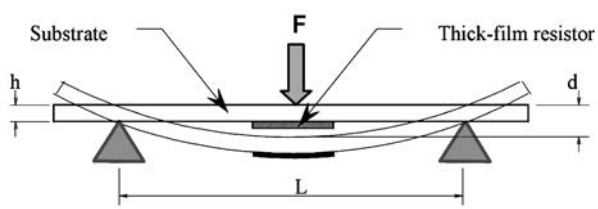

Fig. 2. Principle of bridge measurement method. L is the length of the bridge, h is the thickness of the ceramic substrate, and d is the deflection of the substrate.

thick-film resistor eq. (4) can be rewritten for longitudinally and transversally oriented resistors, respectively, as

$$\frac{dR_{\mathrm{L}}}{R_{\mathrm{L}}} = \frac{d\rho_{\mathrm{xx}}}{\rho} + \varepsilon_{\mathrm{xx}} \cdot (1 + v_{\mathrm{c}} + v_{\mathrm{r}}) \tag{15}$$

$$\frac{dR_{\mathrm{T}}}{R_{\mathrm{T}}} = \frac{d\rho_{\mathrm{yy}}}{\rho} - \varepsilon_{\mathrm{xx}} \cdot (1 + v_{\mathrm{c}} - v_{\mathrm{r}}) . \tag{16}$$

Introducing the longitudinal and transverse gauge factors, GF_{L} and GF_{T}, to substitute for $dR_{\mathrm{L}}/(R_{\mathrm{L}}\varepsilon_{\mathrm{xx}})$ and $dR_{\mathrm{T}}/(R_{\mathrm{T}}\varepsilon_{\mathrm{xx}})$ results in the following relations between the resistivity changes and the experimentally obtained gauge coefficients:

$$\frac{d\rho_{\mathrm{xx}}}{\rho} = (GF_{\mathrm{L}} - 1 - v_{\mathrm{c}} - v_{\mathrm{r}}) \cdot \varepsilon_{\mathrm{xx}} \tag{17}$$

$$\frac{d\rho_{\mathrm{yy}}}{\rho} = (GF_{\mathrm{T}} + 1 + v_{\mathrm{c}} - v_{\mathrm{r}}) \cdot \varepsilon_{\mathrm{xx}} . \tag{18}$$

From eq. (11) the resistivity changes in the longitudinal and transversal resistors can be expressed by the relation with the gauge coefficients and strain components as

$$\frac{\Delta\rho_{\mathrm{xx}}}{\rho} = g_{\mathrm{l}} \cdot \varepsilon_{\mathrm{xx}} + g_{\mathrm{t}} \cdot \varepsilon_{\mathrm{yy}} + g_{\mathrm{t}} \cdot \varepsilon_{\mathrm{zz}} \tag{19}$$

$$\frac{\Delta\rho_{\mathrm{yy}}}{\rho} = g_{\mathrm{t}} \cdot \varepsilon_{\mathrm{xx}} + g_{\mathrm{l}} \cdot \varepsilon_{\mathrm{yy}} + g_{\mathrm{t}} \cdot \varepsilon_{\mathrm{zz}} . \tag{20}$$

By substituting the resistivity changes $d\rho_{\mathrm{xx}}/\rho$ and $d\rho_{\mathrm{yy}}/\rho$ from eqs. (17) and (18) in eqs. (19) and (20), and then expressing the gauge coefficients g_{l} and g_{t}, the following relations between the gauge coefficients and the experimentally obtained gauge factors are derived:

$$g_{\mathrm{l}} = \frac{GF_{\mathrm{L}}(1 - v_{\mathrm{r}}) + GF_{\mathrm{T}}(v_{\mathrm{c}} + v_{\mathrm{r}})}{(1 + v_{\mathrm{c}})(1 - v_{\mathrm{c}} - v_{\mathrm{r}})} - 1 \tag{21}$$

$$g_t = \frac{GF_T + v_c GF_L}{(1 + v_c)(1 - v_c - v_r)} + 1. \quad (22)$$

Assuming that the thick-film resistor and substrate materials are compatible, i.e., that no interaction occurs between the materials during firing, which would result in nonhomogenous resistor regions, eqs. (21) and (22) allow us to calculate the gauge coefficients for any combination of a thick-film resistor and substrate materials from previously obtained *GF*s.

2.3.1 *Experimental results*

To evaluate both GF_L and GF_T using the same experimental set-up, two different test patterns with appropriately oriented thick-film resistors were designed, as presented in Fig. 3. All the conventionally shaped resistors are of the same dimensions: L= W=1.6 mm and a thickness of 14 μm. The design of the test patterns was based on the results of the preliminary FE analysis, which revealed the strain components on the surface of the bent substrate and suggested appropriate positions for the thick-film resistors that allow consistent measurements in accordance with eqs. (21) and (22).

Since the expressions were derived assuming that $\varepsilon_{yy}=-v_c \cdot \varepsilon_{xx}$ and $\varepsilon_{zz}=-v_r \cdot \varepsilon_{xx}$, it was important for the design to ensure the same conditions within the experimentally treated test patterns. To maintain consistent conditions, the test thick-film resistors had to be located at the proper positions on the substrate, depending on the aspect of the measurement set-up. A preliminary FE analysis had shown that, in the case of the three-point bending experimental set-up, the conditions in eq. (14) can be fulfilled for resistors that are moved from the middle of the bridge by at least quarter of the length of the bridge. For this reason, only the test resistors positioned at the appropriate positions on the bridge were treated in the evaluation. According to the test patterns in Fig. 3, GF_L was evaluated from measurements of the resistors R_1 and R_5, while the resistors R_2–R_4 were used for model-validation purposes. To evaluate GF_T, the resistor R_6 was measured and resistor R_8 was used for test purposes. The experimentally obtained gauge factors, GF_L and GF_T, and the calculated gauge coefficients, g_l and g_t, for different thick-film resistive materials printed and fired on different ceramic substrates are shown in Table 1. The two thick-film resistor materials are denoted material A and material B.

The data entered for GF_L and GF_T are the mean parameter values obtained from measurements on several test samples. The maximum deviation of the experimental *GF*s from the specified mean values was less than ± 4%. The accuracy of the gauge coefficients evaluated was assessed to be ± 5%. As evident from Table 1, the difference between the longitudinal and transversal gauge coefficients, which were obtained for thick-film material A, is less than the accuracy of the calculated data. This indicates that material A exhibits isotropic piezoresistive properties. In the case of thick-film material B, the longitudinal gauge coefficient is to some extent higher than the transversal gauge coefficient, indicating anisotropic piezoresistive properties.

Furthermore, the results presented in Table 1 show that both thick-film resistor materials printed and fired on alumina and zirconia substrates have almost the same gauge

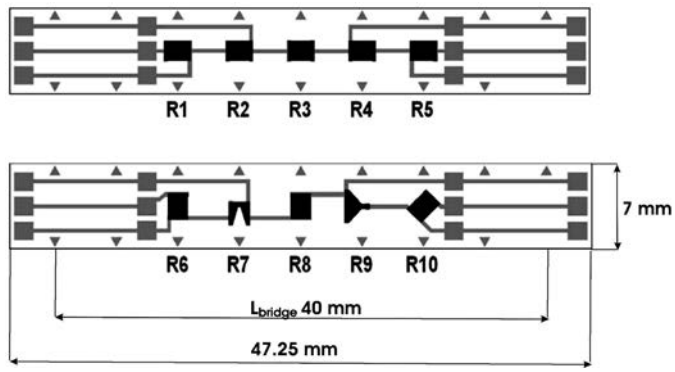

Fig. 3. Test patterns for measurements of GF_L (upper) and GF_T (lower). The nominal resistances of the resistors R_1–R_6, R_8 and R_{10} are 10 kΩ for paste A and 3 kΩ for paste B.

Table 1
Experimentally obtained gauge factors and calculated gauge coefficients for different combinations of thick-film resistor and ceramic materials. Resistor materials: A (DuPont 2041) and B (ESL 3414B); Substrates: Alumina (96% Al_2O_3), LTCC (DuPont 951), Zirconia (Y-ZTP-tetragonal ZrO_2).

Substrate / Resistor material			Gauge factors		Gauge coefficients		$(g_l-g_t)/g_l$ (%)
	v_c	v_r	GF_L	GF_T	g_l	g_t	
Alumina / A	0.23	0.25	10.5	7.4	16.9	16.4	3
LTCC / A	0.17	0.25	8.2	5.6	11.6	11.4	2
LTCC / A-cofired	0.17	0.25	7.9	5.2	11.0	10.6	3
Zirconia / A	0.28	0.25	9.9	6.6	17.2	16.5	4
Alumina / B	0.23	0.25	19.1	11.3	29.8	25.5	15
LTCC / B	0.17	0.25	18.5	10.9	26.2	21.7	17
LTCC / B-cofired	0.17	0.25	16.7	10.8	24.3	21.1	13
Zirconia / B	0.28	0.25	17.5	9.8	29.4	25.5	13

coefficients: the std. deviation for g_l is 1%, and the std. deviation for g_t is 0.6%. A possible interpretation of such results is that they indicate that these two ceramic substrates do not influence the material properties of the thick-film resistor. A noticeable reduction of the gauge coefficients, which was found for both measured thick-film resistor materials processed on LTCC substrates, is most probably a result of the interaction between the substrate and the resistor material, which influences the material properties. Another possible explanation is that because of the relatively high compliance of the LTCC ceramics, which is more than three times higher than the compliance of the alumina and almost two times higher than that of the zirconia substrates, and similar to or even-higher than the compliance of the thick-film resistor, the clamping-to-the-substrate effect results in smaller strains in the resistor and consequently lower *GF*s. The situation in which the compliance of the substrate is higher than the compliance of the thick-film component is not common in practice and does not agree with our assumptions on which eqs. (21) and (22), aimed at calculating the gauge coefficients, were derived. The relationships governing such cases are beyond the scope of this study. Further analyses of the microstructures and measurements of the elastic properties of the treated thick-film resistors are being performed and should help to reveal these mechanisms.

3. FE Modelling

To verify the results of the evaluation procedure, the FE models for the test patterns presented in Fig. 3 were built using the gauge coefficients from Table 1. To reduce the model size, the conductive connection pads were neglected and a voltage was applied directly to the resistors. A three-point bending test was simulated by constraining the displacement of the substrate along the bridge bearers in the z direction and by applying, in the middle of the bridge, the displacement in the opposite direction, as presented in Fig. 4. Three-dimensional static analyses were performed using the multiphysics capability of Ansys 6. Brick as well as tetrahedral elements defined by nodes having three structural degrees of freedom (DOF) were used for the substrates and coupled-field brick elements having the structure and an electric DOF for the thick-film resistor region.

A user-defined procedure for evaluating the resistance was written as a macro to be used in the postprocessing. By coding eq. (13) in an element and implementing an interactive selection of the resistor's region, a number of the subsequent calculations of the resistance for the thick-film resistor structure under the unchanged mechanical load, and for the different gauge coefficients, were made possible using the same sets of results.

3.1 *Validation of FE model*

The validation of the model was performed in two steps. First, the material models and the macro for the calculation of the resistances were verified by comparing the simulated and measured resistance changes for resistors R_1, R_5, and R_6, which were measured for the evaluation of the gauge coefficients. In the following, the differently positioned and shaped resistors, used only for test purposes and not for the actual parameter estimation, were considered. For an illustration, some of the experimental and simulation results that were obtained for the case of bending the test patterns made on an alumina substrate by 150

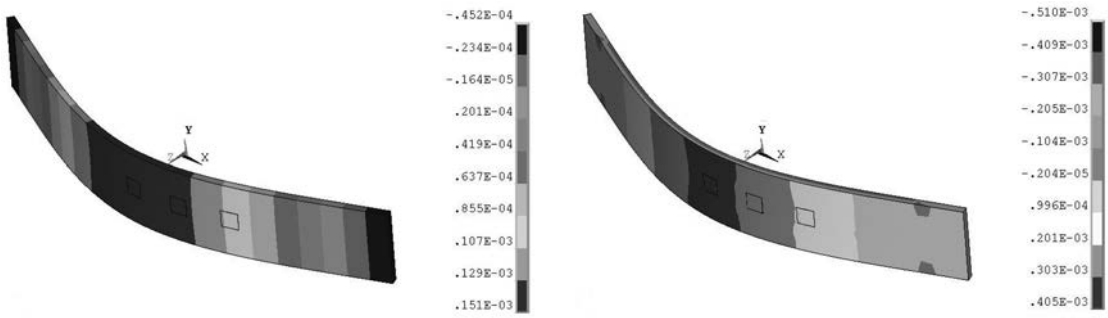

(a) (b)

Fig. 4. (a) Z displacement for test pattern bent by 150 μm, (b) x-component of strain induced as result of bending substrate by 150 μm (right).

μm are collected in Table 2. The simulation results were obtained using a Young's modulus of 340 GPa for the alumina substrate and 98 GPa for the thick-film resistors. Note that since the resistors R_1 and R_5 are of the same dimensions and they are positioned at the same relative positions on the bridge, the measured values for both these resistors are entered as the measurements of R_1. Similarly, the experimental results for the resistors R_2 and R_4 are both considered as the results for R_2.

As is evident from Table 2, the results of the simulations are in very good agreement with the measurements. The differences between the measured and simulated resistance changes are less than 2%, indicating that these deviations are most likely the result of the differences between the particular test resistors or the inaccuracy of the measurements.

In the second step, the sensitivity of the simulation results to the deviation of the experimentally obtained gauge factors was analysed. In fact, our interpretation of the results in Table 1 was that thick-film material A has isotropic piezoresistive properties because the difference between the experimentally obtained gauge coefficients g_l and g_t was smaller than their accuracy. To model such a material, it is normal to specify the same value for both coefficients, i.e., $g_l = g_t = (g_l+g_t)/2$. The question is how accurate would the simulation results be if the mean values for both coefficients are used. The simulations that were performed using the mean value for both gauge coefficients showed slightly lower

values for the resistance changes, but these results were in even better agreement with the measured data. The results obtained for the resistors R_1–R_3 are presented and compared in Table 3.

Table 2
Simulated and measured resistance changes obtained for test samples made on alumina substrate that was bent by 150 μm. The resistances of the resistors R_1–R_6, R_8 and R_{10} obtained from measuring several samples are 9.56 kΩ ± 5% for paste A and 3.05 Ω ±5% for paste B.

Resistor	Resistor paste A		Resistor paste B	
	measured $\Delta R/R$ (%)	simulated $\Delta R/R$ (%)	measured $\Delta R/R$ (%)	simulated $\Delta R/R$ (%)
R_1	0.18	0.18	0.33	0.33
R_2	0.28	0.28	0.52	0.51
R_3	0.40	0.41	0.75	0.73
R_6	0.13	0.13	0.20	0.20
R_8	0.32	0.31	0.49	0.49
R_{10}	0.16	0.16	0.26	0.27

Table 3
Comparison of simulated changes in resistance of thick-film resistors made of material A on alumina substrate, obtained for g_l and g_t from Table 1 (R/R simulated 1) and for $g_l = g_t = (g_l+g_t)/2$ ($\Delta R/R$ simulated 2), with measured data.

Item	$\Delta R/R$ (%) measured	$\Delta R/R$ (%) simulated 1 ($g_l \neq g_t$)	$\Delta R/R$ (%) simulated 2 ($g = g_l = g_t = (g_l+g_t)/2$)	Variation in simulated results (%)	Difference between simulated 2 and measured (%)
R_1	0.181	0.184	0.178	3	1.5
R_2	0.276	0.279	0.270	3	0.4
R_3	0.399	0.412	0.400	3	0.2

4. Conclusions

An approach to numerically modelling the piezoresistivity effect in thick-film resistors was presented, with special emphases on the evaluation of the material model parameters. The combined experimental and mathematical procedure for evaluating the thick-film piezoresistor's gauge coefficients was implemented to determine the gauge coefficients for two commercial thick-film resistor materials deposited on three different ceramic substrates.

The results obtained from evaluating gauge coefficients for different thick-film resistor materials processed on the same ceramic substrates show that some materials exhibit isotropic piezoresistive properties, as in the case of material A, for which the same value for the longitudinal and the transversal gauge coefficients were obtained ($g_l = g_t$). For some other materials, as in the case of material B, the longitudinal gauge coefficient is higher than the transversal gauge coefficient ($g_l > g_t$), indicating an anisotropic material property. Further analyses revealed that both thick-film resistor materials considered in this case study have almost the same gauge coefficients when printed and fired on alumina and zirconia substrates. A possible interpretation of this result is that the materials are compatible and there are no interactions between these ceramic substrates and the thick-film resistors which would influence the material piezoresistive properties. A noticeable reduction in the gauge coefficients that was observed for both thick-film resistor materials processed on the LTCC substrates can be a result of the interaction between the substrate and the resistor material, which results in changes to the material properties. Another possible explanation of this effect is that the compliance of the LTCC ceramics is similar to or even higher than the compliance of the thick-film resistor, such that the clamping-to-the-substrate effect results in smaller *GF*s that would normally be expected. This finding offers a new perspective for the advanced analyses of thick-film piezoresistive structures.

To verify the evaluation procedure, FE models of the treated test patterns were built in which experimentally obtained gauge coefficients were used as the material input. The good agreement between the simulations and the measurements validated the model. Comparison of the results of the simulations with the measurements of the test resistors R_2, R_8 and R_{10}, which were not considered for the evaluation of the gauge coefficients, confirmed the regularity of the evaluation procedure and accuracy of the experimental results. Future work will include some thermal aspects related to this problem.

The results presented show that the proposed FE model is capable of providing reliable and accurate simulation results and could be used for numerical analyses aimed at optimizing the design of different pressure-and load-sensing applications.

Acknowledgements

The financial support of the HYB Company and the Slovenian Research Agency is gratefully acknowledged. Some of the results presented were achieved in the context of a joint research project supported by the Slovenian-Polish Intergovernmental Science and Technology Co-operation Program. The authors thank Prof. Kazimierz P. Friedel, Wroclaw University of Technology, for his valuable suggestions and Mr. Mitja Jerlah, HIPOT R&D, for technical support.

References

1 N. M. White and J. D. Turner: Meas. Sci. Technol. **8** (1997) 1.
2 B. Morten, L. Pirozzi, M. Prudenziati and A. Taroni: J. Appl. Phys. **12** (1979) 51.
3 Canali, D. Malavisi, B. Morten, M. Prudenziati and A. Taroni: J. Appl. Phys. **51** (1980) 3282.
4 M. Prudenziati, B. Morten: Hybrid Circuits **10** (1986) 20.
5 A. Amin: Rev. Sci. Instrum. **60** (1989) 3812.
6 A. Amin: Appl. Phys. Lett. **58** (1991) 1446.
7 C. Grimaldi, P. Ryser, S. Strässler: Phys. Rev. B, Condens. Matter **64** (2001) 1.
8 C. Grimaldi, P. Ryser, S. Strässler: J. Appl. Phys. **90** (2001) 322.
9 M. Hrovat et al.: J. Mater. Sci. Lett. **13** (1994) 992.
10 D. Belavič, M. Hrovat, M. Pavlin and S. Gramc: Proc. European Microelectronics and Packaging Conference 2001 (Strasbourg, 2001) p. 103.
11 D. Belavič, M. Hrovat, M. Pavlin, M. S. Zarnik: Informacije MIDEM **33** (2003) 45.
12 D. Belavič, M. Hrovat, M. S. Zarnik, A. Bencan, W. Smetana, R. Reicher and H. Homolka: Microelectronics International **20** (2003) 41.
13 D. Belavič, A. Degen, A. Dziedzic, K. P. Friedel, L. J. Golonka, M. Hrovat, J. Kita, M. S. Zarnik and A. Wymysłowski: Proc. European Microelectronics and Packaging Conference & Exhibition (Friedrichshafen, Germany, 2003).
14 M. S. Zarnik, D. Belavič, K. P. Friedel and A. Wymysłowski: IEEE Trans. on Components and Packaging Technologies **27** (2004) 668.
15 A. Wymysłowski, M. S. Zarnik, K. P. Friedel and D. Belavič: Proc. Int. Conference Eurosime 2004 (Brussels, 2004) p. 359.